

# CHANGING THE BEHAVIOR OF PARAMETRIC RESONANCE IN MEMS OSCILLATORS BY TUNING THE EFFECTIVE CUBIC STIFFNESS

Wenhua Zhang, Rajashree Baskaran and Kimberly L. Turner

Department of Mechanical & Environmental Engineering, University of California at Santa Barbara  
Engineering II Bldg., Room 2355, Santa Barbara, CA 93106-5070, USA.

Telephone: 1-805-893-7849 Fax: 1-805-893-8651 E-mail: whzh@enr.ucsb.edu

## ABSTRACT

Nonlinearity plays a critical role on the behavior of oscillators operating in the parametric resonance mode. Here, we study the effects of Effective Nonlinear Parameter, (effective cubic stiffness),  $\gamma_{3eff}$ , on the behavior of parametric resonance in a micro electro mechanical oscillator. The value of  $\gamma_{3eff}$  can be tuned by changing the amplitude of applied voltage. Varying the sign of  $\gamma_{3eff}$  can switch bi-stable area from one side of the parametric resonance area to the other side. Both experiment and analysis show this switch and the results agree very well with each other.

## INTRODUCTION

Micro and nano-scale oscillators have found numerous applications in recent years with the advancement of fabrication and integration technologies. Electromechanical filters[1], biological and chemical sensing[2, 3], force sensing[4, 5] and scanning probe microscopes[6] are a few applications. As technology allows for smaller scale features (hence decreasing amplitudes of motion), mechanical to electrical transduction becomes more and more difficult. Thus, mechanical domain parametric amplification schemes[7-9] are attractive. Parametric amplification schemes additionally have good noise rejection and broad bandwidths of operation.

In this paper, we demonstrate how in a particular design of the electrostatic drive combs and mechanical springs, we can tune the effective cubic stiffness, thereby obtaining a wide range of qualitatively varying frequency responses. We focus on how tuning the effective cubic stiffness affects the parametric resonance characteristics of a micro oscillator. Parametrically driven oscillators show promise as filters and with this technology a single oscillator can be tuned to function as low pass, high pass or band pass filter. There is very good agreement with perturbation analysis of the model. This in turn offers tangible design guidelines to engineer the response characteristics like bandwidth and shape of the response in terms of the design and operating parameters.

We have presented a study of parametric resonance in a MEM oscillator with cubic mechanical and electrostatic force terms elsewhere[10]. A 2:1 sub-harmonic resonance (first order parametric resonance) can be generated in an electro statically actuated oscillator with time varying effective stiffness. The dynamic response of the oscillator can be understood to a good degree when modeled with a non-linear Mathieu equation[10, 11]. We have shown that the effective cubic nonlinearity with contributions from the mechanical constraints and electrostatic fringing field plays an important role in the dynamic response of the oscillator.

## DEVICE

The oscillator under study is fabricated by S.G. Adams[12] using SCREAM[13], a bulk micro-machining technique, for the independent tuning of linear and cubic stiffness terms (Fig. 1). The area of the device is about  $500 \times 400 \mu m^2$ . It has two sets of parallel interdigitated comb finger banks on either end of the backbone and two sets of non-interdigitated comb fingers on each side. The four crab-leg beams provide elastic recovering force for the oscillator. The springs, backbone and the fingers are  $\sim 2 \mu m$  wide and  $\sim 12 \mu m$  deep. Either the interdigitated or the non-interdigitated comb fingers may be used to drive the oscillator.

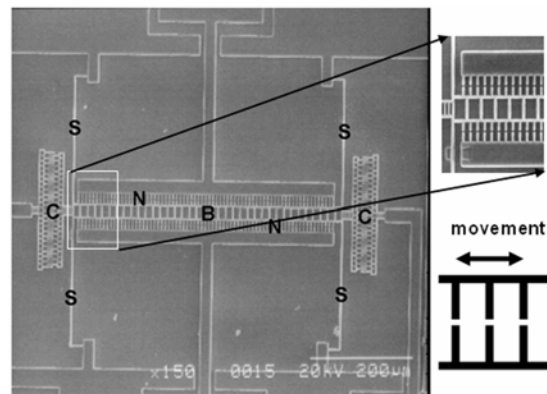


FIG. 1 A Scanning Electron Micrograph of the oscillator. Note the crab-leg beam springs (S), the two sets of interdigitated comb finger banks (C) on both ends of backbone (B) and non-interdigitated comb fingers (N) on each side of backbone (B).

## THEORY

When electrical signal is applied between the non-interdigitated comb fingers and the oscillator, the electrostatic force generated depends on the position of the oscillator. In the experiments presented here, we use a square rooted AC voltage signal ( $V_A (1+\cos 2\omega t)^{1/2}$ ) in order to isolate the parametric response from that of the direct harmonic response[7]. Under such a drive voltage, the equation of motion could be written in normalized form as follows:

$$\frac{d^2x}{d\tau^2} + \alpha \frac{dx}{d\tau} + (\beta + 2\delta \cos 2\tau)x + (\delta_3 + \delta_3' \cos 2\tau)x^3 = 0 \quad (1)$$

$$\text{where } \alpha = \frac{2c}{m\omega} \quad \beta = \frac{4(k_1 + r_1 V_A^2)}{m\omega^2} \quad \delta = \frac{2r_1 V_A^2}{m\omega^2}$$

$$\delta_3' = \frac{4r_3 V_A^2}{m\omega^2} \quad \delta_3 = \frac{4k_3 + 4r_3 V_A^2}{m\omega^2}$$

and  $m$ ,  $k_1$  and  $k_3$  are the mass, linear and cubic mechanical stiffness of the oscillator,  $c$  is the velocity proportional damping coefficient,  $r_1$  and  $r_3$  are linear and cubic electrostatic stiffness and  $\tau = \omega t$  is normalized time variable. The electrostatic force is modeled here as

$$F_e(x, t) = -(r_1 x + r_3 x^3) V_A^2 (1 + \cos(2\omega t)) \quad (2)$$

We use a two-variable perturbation method [11] to analyze Equation (1). The detailed analysis is presented elsewhere[10], only the relevant results are discussed here. When the driving frequency is about two times the first resonant mode frequency of the oscillator, and driving voltage amplitude above a critical value, 2:1 sub-harmonics are generated. The amplitude and phase of this response within this range of frequencies is given by

$$R^{*2} = -\frac{4}{3\gamma_{3eff}} (\beta_1 + \cos(2\theta^*)) \quad (3)$$

$$\theta^* = 0, \frac{\pi}{2}, \pi, \frac{3\pi}{2} \quad (4)$$

where  $\gamma_{3eff}$  is the ENP (Effective Nonlinearity Parameter) of the system, a sum of contributions from cubic mechanical stiffness, which is fixed for a particular beam design and voltage dependant cubic electrostatic stiffness.

$$\gamma_{3eff} = \frac{1}{r_1 V_A^2} (2k_3 + \frac{10}{3} r_3 V_A^2) \quad (5)$$

This result is schematically represented in Fig. 2. The solution characteristics of Equation (3) depend on the sign of ENP. Let us assume the ENP is negative. In this case of  $\theta^* = 0$  and  $\pi$ ,  $R^{*2} = -\frac{4(\beta_1 + 1)}{3\gamma_{3eff}}$ , a

nontrivial stable solution exists at  $\beta_1 > -1$  and the trivial solution is unstable. When  $\theta^* = \pi/2$  and  $3\pi/2$ ,  $R^{*2} = -\frac{4(\beta_1 - 1)}{3\gamma_{3eff}}$ , another

nontrivial (unstable) solution exists and the trivial solution becomes stable, at  $\beta_1 > 1$ . There are two stable solutions at  $\beta_1 > 1$ , so area III is a bi-stable area. If ENP is positive, these two solutions will exist at  $\beta_1 < -1$  and bi-stable area occurs at area I. The responses are mirrored about a vertical axis at  $\beta_1 = 1$  and characteristics of area I and III are swapped. The growth of  $R^*$  with respect to  $\beta$  in different areas is also schematically shown in Fig. 2, where the solid line represents stable solution and dashed line represents unstable solution. Since  $\beta_1 = \pm 1$  corresponds to transition curves from stable to unstable areas in  $\beta$ - $\delta$  plane, bifurcation occurs when we quasi-statically vary frequency of the input voltage across the transition curve.

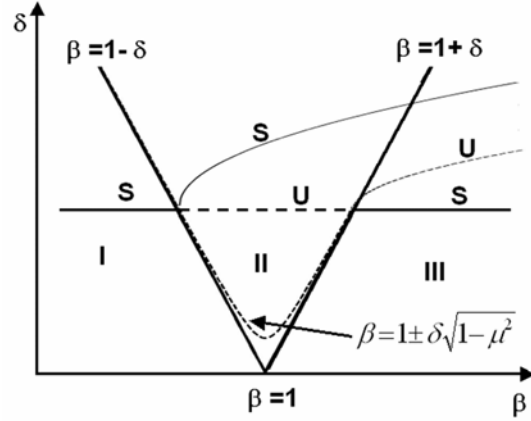


FIG. 2 Schematic characteristics of the solution of the first order parametric resonance.

For the oscillator in our study, boundary element (electrostatic force calculation) and finite element (mechanical stiffness calculation) numerical simulation results show that the values of electrostatic stiffness parameters  $r_1$  and  $r_3$  are  $3.3e-3 \mu N V^{-2} / \mu m$  and  $-0.98e-3 \mu N V^{-2} / \mu m^3$  and mechanical cubic stiffness  $k^3$  is  $0.0437 \mu N / \mu m^3$ . By varying the applied voltage, the value of ENP can be tuned and even switched from positive to negative (see Fig. 3). It should be noted that the figure is a simulation result and does not exactly match the experimental results.

Based on these values, we use numerical method to solve equation (3). The results are shown in Fig. 4. The amplitude of motion,  $R^*$ , is calculated at a low voltage ( $V_A = 6$  V) and a high voltage ( $V_A = 25$  V) respectively. Referring to Fig. 3,  $\gamma_{3eff}$  is positive at  $V_A = 6$  V, while  $\gamma_{3eff}$  is negative at  $V_A = 25$  V. Bi-stable

area switches from right side to left side.

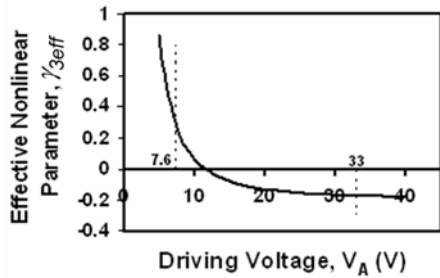


FIG. 3 The effective nonlinear parameter as a function of the driving voltage amplitude  $V_A$ . Note that the sign of effective nonlinear parameter can be switched from positive to negative by changing applied voltage.

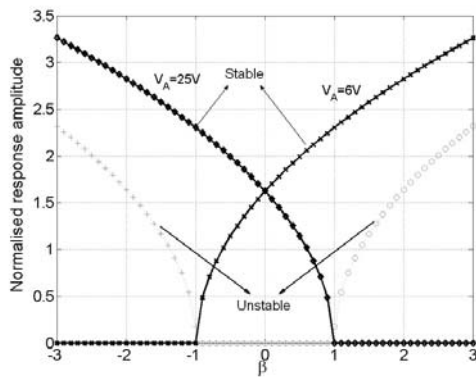


FIG. 4 Numerical simulation results of the first order parametric resonance at different voltages (6 V and 25 V) in  $\beta$ - $\delta$  plane. Note the other two solutions are unstable and cannot be observed in the experiment.

## EXPERIMENTS

The experiments reported here are performed in a multi-dimensional MEMS motion characterization setup[14], as shown in Fig.5. The oscillator is placed in a vacuum chamber with an ambient pressure of  $\sim 7mTorr$ . The in-plane motion is detected by a Laser Doppler Vibrometer (Polytec OFV-501/3001) through a  $45^\circ$  mirror. Velocity and displacement signals are recorded and analyzed through a Spectrum Analyzer (HP89470A) and an Oscilloscope (TDS 420 A).

To actuate parametric resonance, voltage signal is applied between the non-interdigitated comb fingers and the oscillator. A square rooted AC signal is used to avoid coupling with harmonic resonance. At  $7.6V$ ,  $23.8V$  and  $33V$ , the frequency responses of parametric resonance are shown in Fig. 6, 7 and 8 respectively. Frequency is swept up (increasing) and down (decreasing) to capture the bi-stable

characteristics of parametric resonance. Fig. 6, 7 and 8 show the change in the frequency response of the parametrically excited oscillators, corresponding to the value and sign of ENP. At a lower voltage ( $7.6V$ ),  $ENP > 0$ , bi-stable area occurs at the right side of parametric resonance area. When the applied voltage is increased to a higher voltage ( $33V$ ),  $ENP < 0$ , bi-stable area occurs at the left side. Fig. 7 corresponds to an ENP value  $\sim 0$  and we see that there are bi-stable areas on either side of the parametric resonance area. This is not very surprising given that there should be a transition of the bi-stability from region I to region III with tuning of the ENP.

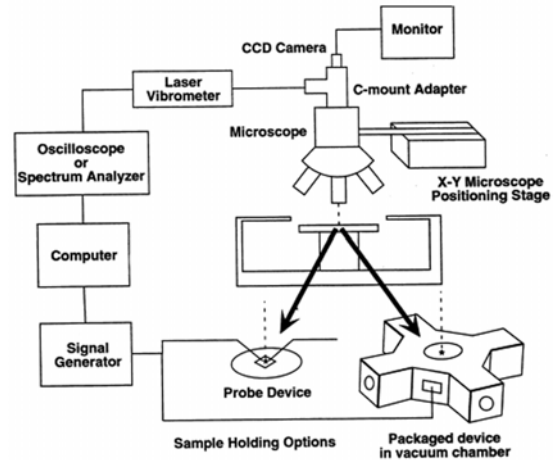


FIG. 5 A schematic of characterization setup. The device is put in a vacuum chamber, where temperature and pressure can be adjusted. The motion is detected by a laser vibrometer.

## CONCLUSION

In conclusion, we have demonstrated that tuning the effective non-linear stiffness can drastically change the frequency response of an auto-parametric oscillator. The metric of importance is the ENP. A perturbation analysis of the governing non-linear Mathieu equation sheds light on the effect of cubic nonlinearity on the response. Experimental results agree well with the analysis. It has been demonstrated that the Effective Nonlinear Parameter of the oscillator can be tuned to have frequency responses which can be utilized as low pass, high pass or band pass filter within the region of parametric resonance excitation.

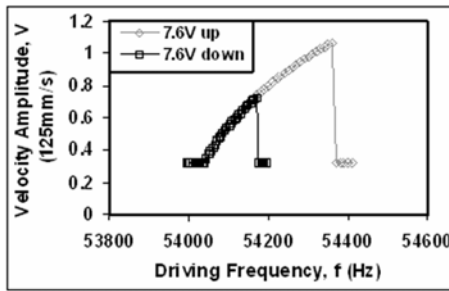


Fig. 6 The frequency response curve of parametric resonance at  $V_A=7.6$  V. Note bi-stable area is located at the right side of parametric resonance

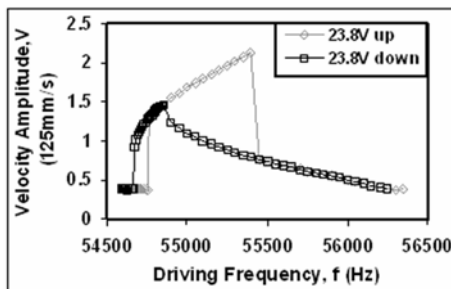


Fig. 7 The frequency response curve of parametric resonance at  $V_A=23.8$  V. Both sides show bi-stable.

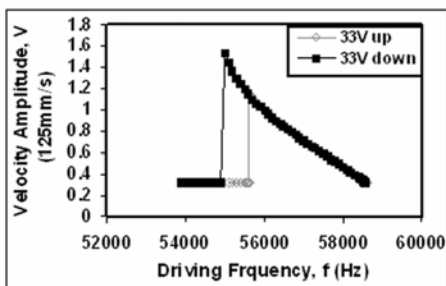


Fig. 8 The frequency response curve of parametric resonance at  $V_A=33$  V. Note bi-stable area is located at the left side of parametric resonance area.

## REFERENCES

- [1] C.T.C. Nguyen, "Micromechanical filters for miniaturized low-power communications," Proc. of Smart Electronics and MEMS Newport Beach, CA, USA, pp. 55-66.
- [2] B. Ilic, D. Czaplewski, H.G. Craighead, P. Neuzil, C. Campagnolo, and C. Batt, "Mechanical resonant immunospecific biological detector," Applied Physics Letters, vol. 77, pp. 450-452, 2000.
- [3] M.K. Baller, H.P. Lang, J. Fritz, C. Gerber, J.K. Gimzewski, U. Drechsler, H. Rothuizen, M. Despont, P. Vettiger, F.M. Battiston, J.P. Ramseyer, P. Fornaro, E. Meyer, and H.J. Guntherodt, "A cantilever array-based artificial nose," Proc. of International Conference on Scanning Probe Microscopy, Cantilever Sensors and Nanostructures, Seattle, WA, USA, 30 May-1 June 1999, pp. 1-9.
- [4] T.D. Stowe, K. Yasumura, T.W. Kenny, D. Botkin, K. Wago, and D. Rugar, "Attonewton force detection using ultrathin silicon cantilevers," Applied Physics Letters, vol. 71, pp. 288-290, 1997.
- [5] T. Kenny, "Nanometer-scale force sensing with MEMS devices," IEEE Sensors Journal, vol. 1, pp. 148-157, 2001.
- [6] D. Rugar, C.S. Yannoni, and J.A. Sidles, "Mechanical detection of magnetic resonance," Nature, vol. 360, pp. 563-566, 1992.
- [7] K.L. Turner, S.A. Miller, P.G. Hartwell, N.C. MacDonald, S.H. Strogartz, and S.G. Adams, "Five parametric resonances in a microelectromechanical system," Nature, vol. 396, pp. 149-152, 1998.
- [8] A. Olkhovets, D.W. Carr, J.M. Parpia, and H.G. Craighead, "Non-degenerate nanomechanical parametric amplifier," Proc. of Technical Digest. MEMS 2001. 14th IEEE International Conference on Micro Electro Mechanical Systems, Interlaken, Switzerland, 21-25 Jan. 2001, pp. 298-300.
- [9] J.P. Raskin, A.R. Brown, B. Khuri-Yakub, and G.M. Rebeiz, "A novel parametric-effect MEMS amplifier," Journal of Microelectromechanical Systems, vol. 9, pp. 528-537, 2000.
- [10] W. Zhang, R. Baskaran, and K.L. Turner, "Effect of cubic nonlinearity on auto-parametrically amplified resonant MEMS mass sensor," Sensors and Actuators A (Physical), vol. In Press, 2002.
- [11] R.H. Rand, Lecture Notes on Nonlinear Vibrations, version 34a: Available online at <http://www.tam.cornell.edu/randdocs/>, 2000.
- [12] S.G. Adams, F.M. Bertsch, K.A. Shaw, and N.C. MacDonald, "Independent tuning of linear and nonlinear stiffness coefficients [actuators]," Journal of Microelectromechanical Systems, vol. 7, pp. 172-180, 1998.
- [13] N.C. MacDonald, "SCREAM microelectromechanical systems," Microelectronic Engineering, vol. 32, pp. 49-73, 1996.
- [14] K.L. Turner, "Multi-dimensional MEMS motion characterization using laser vibrometry," Proc. of Transducers'99 The 10th International conference on solid-state Sensors and Actuators, Digest of Technical Papers, Sendai, Japan, 7-10 June 1999, pp. 1144-1147.